Manufacturing Process Models for Thermoplastic Composites

SUSAN C. MANTELL AND GEORGE S. SPRINGER
Department of Aeronautics and Astronautics
Stanford University
Stanford, CA 94305

ABSTRACT: Models were developed which simulate the processing of thermoplastic matrix composites. The models relate the applied temperature, pressure, speed, and time to the temperature, crystallinity, consolidation, interlaminar bonding, and residual stresses and strains inside the composite. The formulations follow the models proposed by Springer, Loos, and their coworkers for manufacturing plates in a press or in an autoclave, but were extended to include cylindrical geometries, variations in the applied temperatures and pressures with position and time, and rapid bonding. These extensions make the models applicable to the manufacture of plates by tape laying and to filament winding of cylinders. These models were incorporated into a user friendly computer code which can be used to generate numerical results and to select the appropriate processing conditions for processing thermoplastic composite plates 1) in an autoclave, 2) in a press, or 3) by tape laying, and 4) for filament winding thermoplastic composite cylinders.

1. INTRODUCTION

THREE TYPES OF processes have generally been used to produce thermoplastic composite structures. In the first, the entire structure is arranged in the required shape. Then, inside either an autoclave or a press, suitable temperatures and pressures are applied to the pre-assembled structure. In the second process, tapes containing a matrix-fiber mixture are laid in a prearranged pattern, and the required processing temperatures and pressures are applied continuously as the tape is being laid. In the third process, either fiber tows impregnated with matrix or narrow tapes containing fibers and matrix are wound on a mandrel. Temperature and pressure are then applied either continuously as the tows or tapes are being wound or after the winding of the entire structure has been completed. In all of these processes it is important that the proper temperatures and pressures be applied, otherwise the composite properties may suffer; the crystallinity may be nonuniform, the plies may not be consolidated, and the residual stresses and strains may be unacceptable.

The difficulties encountered in manufacturing thermoplastic matrix composites

could best be overcome by the use of analytic models. Models simulating the manufacturing process may shed light on the major phenomena which take place during processing, indicate ways in which the process may be modified and improved, and provide the appropriate processing conditions. Recognizing the importance of models, several investigators presented models for the processing of thermoplastics. The earliest of these pertained to fabrication of parts in an autoclave or in a press [1–6]. Only recently have models been proposed of the tape laying and the filament winding processes as applied to thermoplastic composites. The models for tape laying have generally addressed the problem of heating the material, with little or no attention paid to the problems of crystallinity, consolidation, or residual stresses [7–12]. Models describing filament winding of thermoplastics have been proposed by Cirino [13], by Brage and Lamrell [14], and by Guceri and his co-workers [15–17]. The major emphasis in these models was on the heat transfer process during filament winding. Cirino looked at the problem where the entire surface of the cylinder was at uniform heat flux. Guceri et al., simulated the heating of the surface by a laser, and analyzed the heat transfer process due to spot heating on the surface. None of these investigators included directly either crystallization or consolidation in their models.

The goal of this investigation was to develop models which describe the manufacture of thermoplastic composites either in an autoclave (or press), by tape laying, or by filament winding. The models are to allow for nonuniform temperature or heat transfer distributions on the composite surfaces, include consolidation, take into account crystallization, and consider residual stresses and strains inside the composite. An additional goal was to write user friendly computer codes for performing the necessary calculations.

2. PROBLEM STATEMENT

A flat plate or a circular cylinder, made of fiber reinforced thermoplastic matrix composite, is being manufactured by applying heat and pressure to the material. It is desired to find the following parameters inside the composite as functions of position and time: 1) temperature, 2) crystallinity, 3) degree of bonding, and 4) residual stresses and strains. Three specific problems were studied, and these are described below.

Autoclave or Press; Flat Plate — Uniform Pressure and Temperature

A flat plate consists of n layers (plies) of thermoplastic prepreg tape. Each layer may be made of a different material. The plate is "thin" so that its thickness H is small compared to its length L and width W ($H/L \ll 1$; $H/W \ll 1$). The composite plate is placed between two platens (Figure 1). These may be the platens in a press or may simulate the tool plate, the bleeder, the breather, and the vacuum bag in an autoclave. Hence, the process described below is applicable to processing either in an autoclave or in a press.

Heating (or cooling) and pressure are applied to the composite by means of the platens. The thermal behavior is specified by either prescribing the temperatures on the surfaces of the composite (T_{st} and T_{sb}) or on the outside surfaces of the
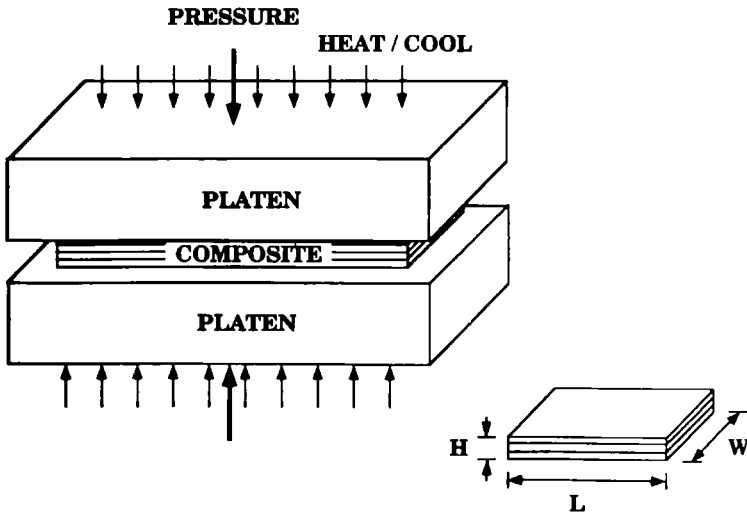
Figure 1. Illustration of the press.

platens (T_t and T_b), or the heat fluxes (q_t and q_b) to the platen surfaces (Figure 2). The temperatures or the heat fluxes may be different on the two sides and may vary with time, but they must be uniform across each surface. The temperatures or heat fluxes may be such that heat is transferred to or from the surface. Pressure P is also applied to the composite by the two platens (Figure 1). This pressure (which may be applied by either a press or in an autoclave) may also vary with time but is uniform across the surface.
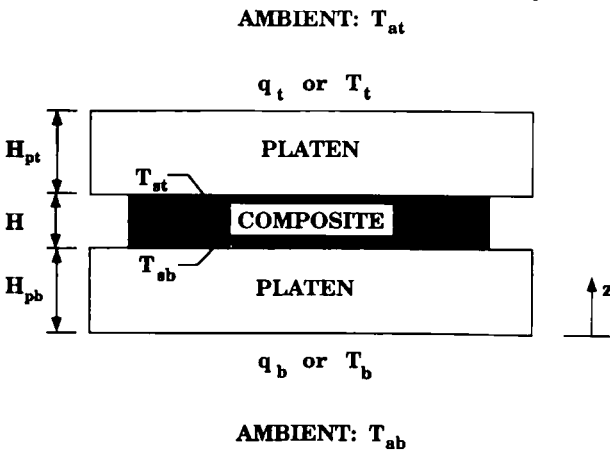

Figure 2. Thermal boundary conditions for the press.

Tape Laying; Flat Plate—Nonuniform Pressure and Temperature

As in the previous problem, we consider a "thin" ($H/L \ll 1$; $H/W \ll 1$) flat plate made of n layers of thermoplastic prepreg tape. Each layer may be made of a different material. The composite plate is placed on a flat "tool plate" which may be either heated or cooled (Figure 3). The heating and cooling of the tool plate are described by specifying either the temperature T_b at or heat flux q_b to the tool plate's bottom and side surfaces (Figure 4).

A moveable head, consisting of heaters, coolers, and rollers, is mounted above the composite plate. The heaters and coolers heat or cool the plate from above, while the rollers apply a known amount of pressure P to the plate. The head moves with constant speed V, exposing parts of the composite plate to the head. The temperature T_{se} or heat flux q_{se} at the composite's edges are assumed to be uniform and constant (Figure 4). The heating and cooling of the composite's top surface are described by specifying either the composite's surface temperature T_{st} or the heat flux q_{st} to or from the surface. However, the specified top surface temperature or specified top surface heat flux may vary in an arbitrary manner along the length (i.e. in the direction in which the head moves). Thus the temperature and pressure may vary with time and position along the length inside the composite (x direction), and these lengthwise variations are included in this investigation. However, the temperature and pressure distributions across the width are taken to be uniform.

The thickness of the composite H changes as successive plies are being laid down. The heat and pressure may be applied continuously during the tape laying process or may be applied after several plies have been laid down.

Filament Winding; Nonuniform Pressure and Temperature

A cylinder is made of layers of thermoplastic prepreg tows by placing bands of tows onto a rotating mandrel (Figure 5). The material in each layer may be different. The mandrel is represented by a hollow cylinder with a uniform effective wall thickness.

The tows are deposited under tension (initial fiber tension F_0) by a crosshead moving at speed V parallel to the mandrel axis. The mandrel angular speed is ω. The fiber orientation in a layer (winding angle) is ϕ_0. During winding, the outer surface of the composite may be either heated or cooled. Additionally, pressure may be applied to this surface. Heat and pressure may be applied continuously at the location where the fiber bands are being laid down (Figure 5) or after the winding of one or more layers is complete (Figure 6). When heat and pressure are applied locally, the process is similar to tape laying described above.

When heat and pressure are applied along the entire length of the cylinder, then we assume that these vary around the circumference (but not in the axial direction) and also may vary with time. This latter condition implies that heating, cooling and pressure may be applied at any time after one, two or more layers have been wound. The applied pressure, heating, and cooling are known. Heating and cooling may be applied at the outer surface of the composite cylinder and at the inner surface of the mandrel. The heat transfer at the outer surface of the
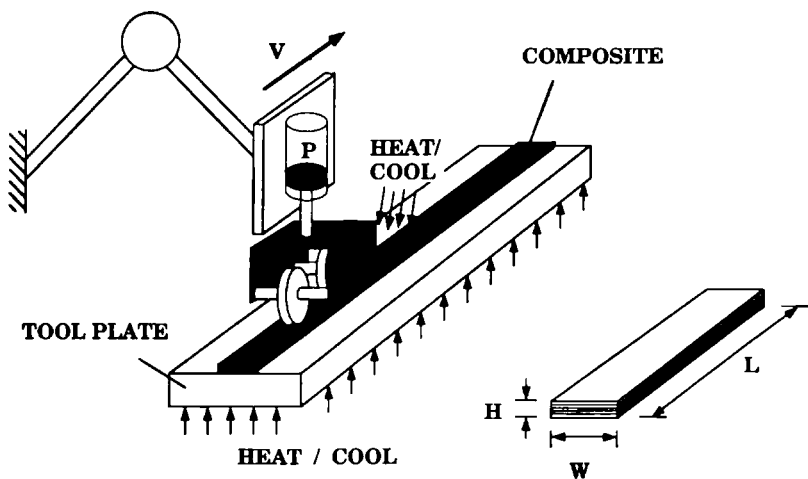
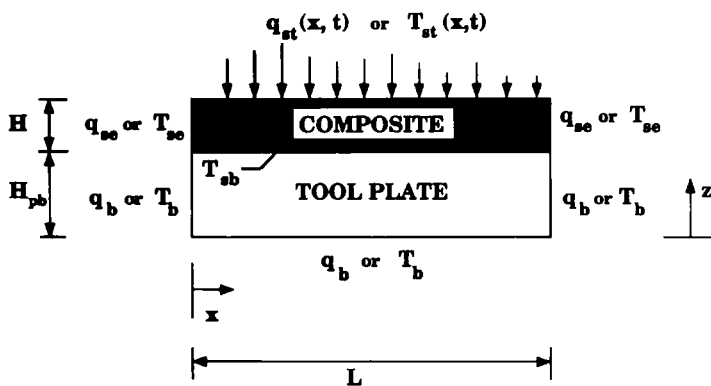**Figure 3.** *Illustration of the tape laying apparatus.*

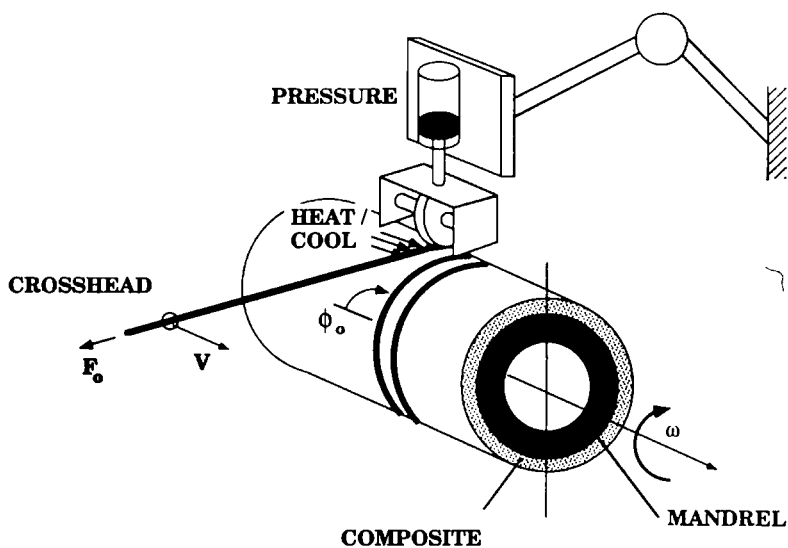**Figure 4.** *Thermal boundary conditions for the tape laying process.*

Figure 5. *Local application of heat and pressure during the filament winding process.*
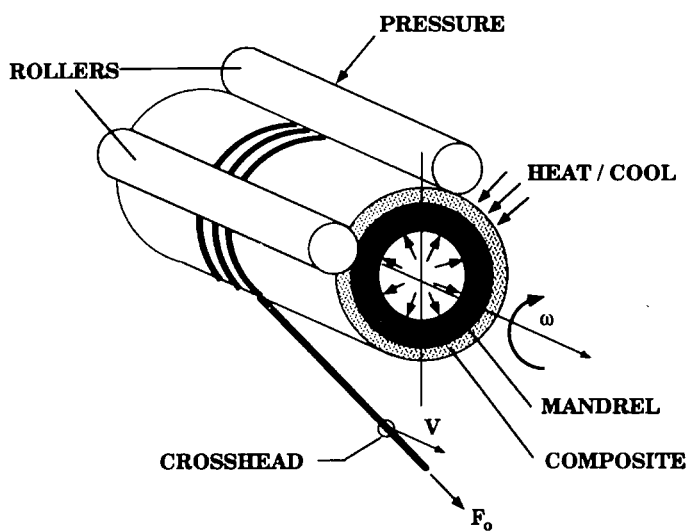

Figure 6. *Application of heat and pressure along the length of the cylinder in the filament winding process.*

2353

cylinder can be specified by prescribing either the composite's surface temperature T_{so} or the heat flux q_{so}. These may vary in the circumferential direction and with time (Figure 7). The conditions inside the mandrel can be specified by prescribing either the inside mandrel surface temperature T_{si} or the heat flux q_{si} to or from this surface. The temperature T_{si} and the heat flux q_{si} may vary with time but must be uniform across the entire inner mandrel surface. As in the case of tape laying, the thickness of the composite changes as successive layers are being wound. The heat and pressure applied may be applied continuously or after the winding of one or more layers is complete.

Objectives

The aim of this study is to establish models which, for a given problem, provide the temperature, crystallinity, degree of bonding, and residual stresses and strains inside the composite. Following previous approaches used in simulating autoclave curing and filament winding processes [2,18–20], the present model is divided into three submodels 1) thermo-chemical, 2) consolidation and bonding, 3) stress and strain. In the following sections, each of these submodels is described separately. Note, however, that the submodels are coupled and must be solved simultaneously.

The thermochemical submodel is based on Lee and Springer's model [2]. The formulation was extended to include cylindrical as well as flat plate geometries, and variations in surface temperatures and pressures both with position and time. In addition, the model by Maffezzoli et al. [21] for changes in crystallinity during melting has been incorporated into the thermochemical submodel. The consolidation and bonding submodels are based on the analyses of Lee and Springer [2] and Loos and his coworkers [22–24]. The current formulation allows for varia-
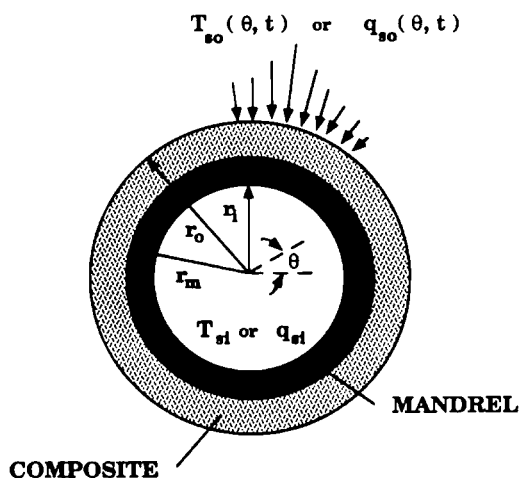

Figure 7. Thermal boundary conditions for the filament winding process.

tions in viscosity with temperature, for variations in pressure with time, and for rapid bonding. The stress-strain submodels are based on laminate plate theory for flat plates [25–27], and on the thermosetting filament winding model of Lee and Springer [19]. However, the latter model was modified to account for changes in crystallinity in the thermoplastic matrix. Finally, the various submodels were incorporated into a computer code, which provides hitherto unavailable solutions to tape laying and filament winding processes.

3. THERMOCHEMICAL SUBMODEL

The thermochemical submodel yields the temperature T, the crystallinity of the matrix c, and the viscosity μ inside the composite as functions of positions and time. The starting point of the analysis is the energy equation which, for the problems under consideration, is

$$\varrho C \frac{\partial T}{\partial t} = \nabla \cdot k \nabla T + \varrho \dot{Q} \tag{1}$$

T is the temperature, ϱ is the density, C is the specific heat, k is the thermal conductivity, and t is time. The ∇ operator is defined subsequently. $\dot{Q}$ is the rate at which heat is generated or absorbed by the composite during heating and cooling, i.e.

$$\varrho \dot{Q} = \varrho_m v_m \frac{dH_m}{dt} + \varrho_f v_f \frac{dH_f}{dt} \tag{2}$$

where ϱ is the density, v is the volume fraction, and H is the heat evolved or absorbed from time $t = 0$ to time t. The subscripts m and f refer to the matrix and the fiber, respectively. Generally, for the fibers H_f is negligible. For a semi-crystalline material the term H_m is related to the crystallinity by [2,28]

$$c = \frac{H_m}{H_u} \tag{3}$$

where H_u is the theoretical ultimate heat of crystallinity. For an amorphous material the rate of heat generation $\dot{Q}$ is zero.

For a flat plate in which the temperature varies only in the lengthwise x and through the thickness z directions (Figures 2 and 4), the energy Equation (1) becomes ($H_f \approx 0$)

$$\varrho C \frac{\partial T}{\partial t} = \frac{\partial}{\partial x}\left(k_x \frac{\partial T}{\partial x}\right) + \frac{\partial}{\partial z}\left(k_z \frac{\partial T}{\partial z}\right) + \varrho_m v_m H_u \frac{dc}{dt} \tag{4}$$

For a cylinder in which the temperature varies only in the radial r and circumferential θ directions (Figure 7) the energy Equation (1) is of the form ($H_f \approx 0$)

$$\varrho C \frac{\partial T}{\partial t} = \frac{1}{r} \frac{\partial}{\partial r} \left(k_r \frac{\partial T}{\partial r} \right) + \frac{1}{r^2} \frac{\partial}{\partial \theta} \left(k_\theta \frac{\partial T}{\partial \theta} \right) + \varrho_m \nu_m H_u \frac{dc}{dt} \tag{5}$$

k_x, k_z, k_r, k_θ are the thermal conductivities of the composite in the direction indicated by the subscripts. If the temperature varies only across the thickness (z direction), the x derivative in Equation (4) and the θ derivative in Equation (5) are zero. Equation (4) applies to the composite as well as to the platens or the tool plate (Figures 2 and 4), while Equation (5) applies to the composite cylinder and to the mandrel (Figure 7). For the platens, the tool plate, and the mandrel, the last term on the right-hand side is zero.

The energy equation contains two unknowns, namely the temperature and the crystallinity. An additional expression is needed to complete the formulation of the problem. This expression is provided by a relationship between the rate of change of crystallinity, the crystallinity, the temperature, and the rate of change of temperature. This relationship can symbolically be expresssed as

$$\frac{dc}{dt} = f_1 \left(c, T, \frac{dT}{dt} \right) \tag{6}$$

Expressions for the function f_1 are given in Appendix A for PEEK composites.

The density ϱ, the heat capacity C, and thermal conductivity $\mathbf{k}$ of the composite may vary with crystallinity and temperature. Expressions relating these properties to crystallinity and temperature are given in Appendix B.

To calculate the temperature and crystallinity the initial and boundary conditions pertaining to the given problem must be specified. The appropriate initial and boundary conditions are discussed subsequently. First, the following general observations are made regarding the boundary conditions.

The conditions at each surface can be specified by prescribing either a) the surface temperature T_s, b) the temperature of the ambient surrounding the surface T_a, or c) the heat flux to the surface q. The ambient temperature is related to the heat flux by

$$q = h(T_s - T_a) \tag{7}$$

where h is the convective heat transfer coefficient. The surface heat flux is related to the surface temperature by

$$q = -k_n \frac{\partial T}{\partial n} \bigg|_s \tag{8}$$

where $\partial T / \partial n |_s$ is the temperature gradient normal to the surface evaluated at the surface, and k_n is the heat conductivity of the material normal to the surface.

It is emphasized that these conditions correspond to heating the surface from the "out-side" as illustrated in Figures 1, 3, 5 and 6. They do not correspond directly to problems in which heat is applied between the layers, as occurs with laser spot heating.

Flat Plate; Uniform Temperature (Autoclave or Press)

When the entire composite plate is processed, the initial temperature of the platens T_{in}^p, and the initial temperature T_{in}^c and initial crystallinity c_{in} of the composite must be specified. The corresponding initial conditions are ($t \leq 0$)

$$T = T_{in}^p \qquad \text{in platens}$$

$$T = T_{in}^c \text{ and } c = c_{in} \qquad \text{in composite} \tag{9}$$

The boundary conditions can be specified either directly at the two surfaces of the composite plate or at the top and bottom platen surfaces (Figure 2). If the boundary conditions on the surfaces of the composite plate are specified, then the relevant boundary conditions are ($t > 0$)

$$T = T_{sb} \quad \text{at} \quad z = H_{pb}$$

$$T = T_{st} \quad \text{at} \quad z = H_{pb} + h \tag{10}$$

where T_{sb} and T_{st} are the temperatures at the composite bottom and top surfaces, respectively. At the outside platen surfaces, either the surface temperature, the heat flux, or the ambient temperature can be specified. When the platen surface temperatures or the heat fluxes are given, the boundary conditions are ($t > 0$)

$$T = T_b \quad \text{or} \quad q = q_b \quad \text{at} \quad z = 0$$

$$T = T_t \quad \text{or} \quad q = q_t \quad \text{at} \quad z = H_{pb} + H + H_{pt} \tag{11}$$

where q is the heat flux and the subscripts b and t refer to the two surfaces illustrated in Figure 2. When the ambient temperatures above and below the platens (T_{at} and T_{ab}) are specified, then the corresponding boundary conditions become ($t > 0$)

$$q = h_b(T_b - T_{ab}) \quad \text{at} \quad z = 0$$

$$q = h_t(T_t - T_{at}) \quad \text{at} \quad z = H_{pb} + H + H_{pt} \tag{12}$$

where h_b and h_t are the convective heat transfer coefficients at the platen surfaces.

Flat Plate; Nonuniform Temperature (Tape Laying)

The thermal conditions applicable to the tape laying process are illustrated in Figure 4. The initial temperature of the tool plate T_{in}^p, and the initial temperature T_{in}^c and initial crystallinity c_{in} of the composite must be specified. Thus the initial conditions are ($t \leq 0$)

$$T = T_{in}^p \qquad \text{in tool plate}$$

$$T = T_{in}^c \text{ and } c = c_{in} \qquad \text{in composite} \tag{13}$$

At time $t > 0$ the temperatures or the heat fluxes at the tool plate and composite surfaces must be specified. For the tool plate, the conditions (heat flux q_b or surface temperature T_b) are taken to be the same and constant on the bottom and on the sides (Figure 4). Thus for the tool plate the boundary conditions are $(t > 0)$

$$T = T_b \quad \text{or} \quad q = q_b \quad \text{at} \quad \begin{cases} 0 \leq x \leq L; & z = 0 \\ x = 0; & 0 \leq z \leq H_{pb} \\ x = L; & 0 \leq z \leq H_{pb} \end{cases} \quad (14)$$

The prescribed temperature or heat flux on top of the composite may vary along the lengthwise x direction and with time. Thus we have

$$T = T_{st}(x,t) \quad \text{or} \quad q = q_{st}(x,t) \quad \text{at} \quad 0 < x < L; \quad z = H_{pb} + H \quad (15)$$

Along the two "short" edges of the composite (see Figure 4), the conditions (q_{se} or T_{se}) are taken to be the same, and to be uniform and constant. The boundary conditions at these edges are $(t > 0)$

$$T = T_{se} \quad \text{or} \quad q = q_{se} \quad \text{at} \quad \begin{cases} x = 0; & H_{pb} < z \leq H_{pb} + H \\ x = L; & H_{pb} < z \leq H_{pb} + H \end{cases} \quad (16)$$

Instead of specifying the heat flux directly, the temperature T_a ambient to any of the surfaces could be prescribed. In this case, the heat flux at the corresponding location is obtained from Equation (7).

Instead of specifying the temperature or heat flux at the bottom surface of the tool plate, the surface temperature of the composite T_{sb} can be prescribed directly. In this case, the boundary conditions given by Equation (14) are replaced by

$$T = T_{sb} \quad \text{at} \quad 0 \leq x \leq L; \quad z = H_{pb} \tag{17}$$

It is reemphasized that the above conditions can be applied while individual layers are being laid down or after every layer has been put in place. In the former case, the composite thickness is not constant, but varies with time.

Filament Winding; Nonuniform Temperature

As noted previously during filament winding heat and pressure can be applied locally (Figure 5) at the position where the tows are being laid down or along the entire length of the cylinder (Figure 6). The thermochemical processes which occur during the former process can be represented by the tape laying submodel given above and are not repeated here. The initial and boundary conditions described in the latter problem (i.e., when heat and pressure are described along the length of the cylinder) are given below.

The thermal conditions for the filament winding process are illustrated in Figure 7. The initial temperature of the mandrel T_{in}^m, and the initial temperature T_{in}^c and initial crystallinity c_{in} of the composite must be specified. These initial conditions are ($t \leq 0$)

$$T = T_{in}^m \qquad \text{in mandrel}$$
$$T = T_{in}^c \text{ and } c = c_{in} \qquad \text{in composite} \qquad (18)$$

In addition to the initial conditions, the temperatures or the heat fluxes at the mandrel inside surface and at the composite cylinder outside surface must be specified at time $t > 0$. At the inside surface of the mandrel, the temperature T_{si} or heat flux q_{si} must be uniform and constant. The corresponding boundary condition is ($t > 0$)

$$T = T_{si} \quad \text{or} \quad q = q_{si} \quad \text{at} \quad r = r_i \qquad (19)$$

where r_i is the mandrel inside surface radius. At the outer surface of the cylinder, either the surface temperature T_{so} or the heat flux q_{so} can be specified (Figure 7). Either of these may vary in the circumferential θ direction and with time. The boundary condition is ($t > 0$)

$$T = T_{so}(\theta, t) \quad \text{or} \quad q = q_{so}(\theta, t) \quad \text{at} \quad r = r_o \qquad (20)$$

where r_o is the composite outside surface radius.

Instead of specifying the heat fluxes or temperatures at the mandrel and cylinder surfaces, the temperature of the surrounding ambient could be prescribed. In this case the heat flux to the surface is to be calculated by Equation (7).

The above conditions can be applied after one or more layers have been wound or after the winding is complete. In the former case, the composite cylinder thickness varies with time.

Summary

Solutions to the energy Equation (4) or (5) together with the appropriate initial and boundary conditions described above provide the temperature and crystallinity inside the composite as functions of position and time. Once the temperature is known, the viscosity μ can be determined provided that the temperature-viscosity relationship for the material is known. The viscosities of PEEK and APC-2/AS4 are given in Appendix A.

4. CONSOLIDATION AND BONDING SUBMODELS

During processing, first the individual plies consolidate and come into intimate contact and then bonding takes place at the contact surfaces. These processes are described below by submodels which are based on the concepts proposed by Loos and his coworkers [6,22–24] and by Lee and Springer [2].

Consolidation

During consolidation the initially irregular ply surfaces (Figure 8) become smooth. Following Lee and Springer this irregular ply surface is replaced by a surface consisting of a series of rectangles (Figure 9). The degree of intimate contact is then defined as

$$D_{ic} = \frac{b}{w_o + b_o} \tag{21}$$

where b_o and b are the initial ($t \leq 0$) and instantaneous (at time t) widths of each rectangular element, respectively, and w_o is the initial distance between two adjacent elements. The volume of each element is constant

$$a_o b_o = ab \tag{22}$$

where a_o and a are the initial and instantaneous heights of each rectangular element. Equations (21) and (22) yield the following expression for the degree of intimate contact

$$D_{ic} = \frac{a_o/a}{1 + w_o/b_o} \tag{23}$$

Referring to Figure 10 it is clear that the law of conservation of mass for a control volume of width $d\xi$ is

$$a \frac{du_\xi}{d\xi} + \frac{da}{dt} = 0 \tag{24}$$

where ξ is the coordinate along the interface and t is time. By assuming that the flow is laminar, we write the average velocity u_ξ as

$$u_\xi = -\frac{a^2}{12\mu_{mf}} \frac{dp}{d\xi} \tag{25}$$

Here μ_{mf} is the rheometric viscosity of the matrix-fiber mixture measured between two parallel platens in shear under adiabatic conditions. P is the absolute pressure at a location inside an element, as shown in Figure 10. Note that P is a function of the position ξ and time t. In the space between two adjacent elements the pressure is P_e which is taken to be equal to the ambient pressure. The edge of the element ($\xi = b/2$) moves with a speed of db/dt. Thus, the boundary conditions corresponding to Equation (25) are ($t > 0$)

$$P = P_e \quad \text{and} \quad u_\xi = \frac{db}{dt} \quad \text{at} \quad \xi = \frac{b}{2} \tag{26}$$
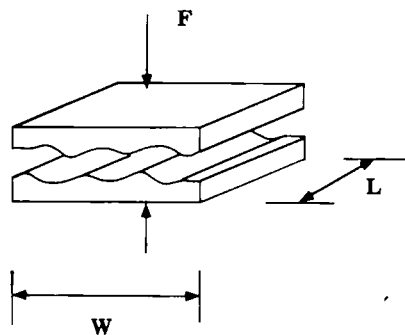
Figure 8. Geometry of the plies prior to consolidation.
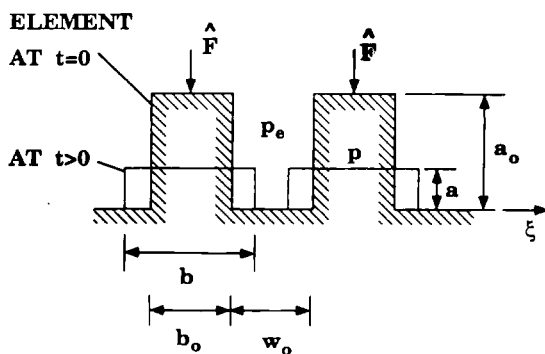

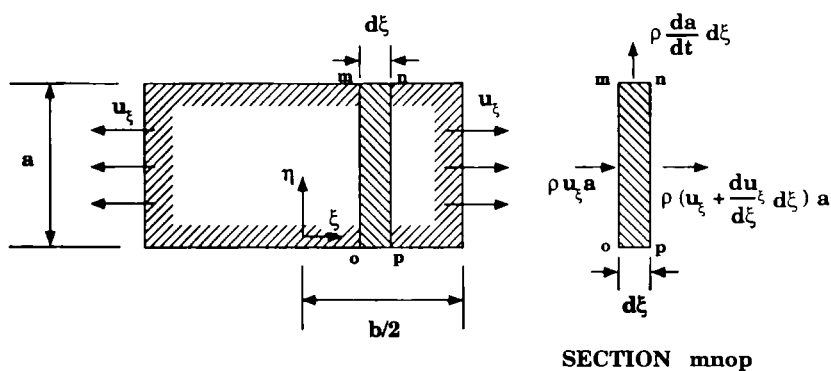**Figure 9.** Rectangular elements representing the uneven surface at time $t = 0$ and $t > 0$.

SECTION mnop

Figure 10. Illustration of one element at time t, and the control volume used in calculating mass flows.

2361

Equations (24)–(26) yield

$$P - P_e = \frac{6\mu_{mf}}{a^3} \frac{da}{dt}\left(\xi^2 - \left(\frac{b}{2}\right)^2\right) \tag{27}$$

The force applied to the ply of length L and width W is F (Figure 8), and the force applied per unit length to one element is

$$\hat{F} = \frac{F}{L} \frac{(b_o + w_o)}{W} = (P_{app})(b_o + w_o) \tag{28}$$

where P_{app} is the applied gauge pressure. The force applied to an element must be balanced by the pressure inside the element

$$\hat{F} = \int_{-b/2}^{b/2} (P - P_e)d\xi \tag{29}$$

Equations (27), (28), and (29) give

$$P_{app}(b_o + w_o) = \int_{-b/2}^{b/2} \frac{6\mu_{mf}}{a^3} \frac{da}{dt}\left(\xi^2 - \left(\frac{b}{2}\right)^2\right)d\xi \tag{30}$$

Integration yields

$$P_{app}(b_o + w_o) = -\mu_{mf} \frac{da}{dt} \frac{b^3}{a^3} \tag{31}$$

By substituting Equation (22) into Equation (31) and integrating with respect to the instantaneous element height a we obtain

$$(b_o + w_o) \int_0^{t_c} \frac{P_{app}}{\mu_{mf}} dt = \frac{(a_o b_o)^3}{5}\left(\frac{1}{a^5} - \frac{1}{a_o^5}\right) \tag{32}$$

Combining Equation (32) together with Equation (23) results in the following expression for the degree of intimate contact

$$D_{ic} = \frac{1}{1 + \dfrac{w_o}{b_o}}\left[1 + 5\left(1 + \frac{w_o}{b_o}\right)\left(\frac{a_o}{b_o}\right)^2 \int_0^{t_c} \frac{P_{app}}{\mu_{mf}}dt\right]^{1/5} \tag{33}$$

where t_c is the time (contact time) during which pressure is applied. This expres-

sion is similar to the one given by Lee and Springer with one notable difference. The Lee and Springer result is for the case where the applied pressure P_{app} and viscosity μ_{mf} are constant, independent of time. Frequently, the second term in the brackets in Equation (33) is large compared to unity. Typical values of this term for press and tape laying applications are shown in Figure 11 [the form of this term for tape laying is defined below by Equation (41)]. When the second term in Equation (33) dominates, the degree of intimate contact may be approximated by

$$D_{ic} \approx \frac{1}{w^*}\left[a^* \int_0^{t_c} \frac{P_{app}}{\mu_{mf}} dt \right]^{1/5} \tag{34}$$

where w^* and a^* are defined as

$$w^* = 1 + \frac{w_o}{b_o} \quad \text{and} \quad a^* = 5w^*\left(\frac{a_o}{b_o}\right)^2 \tag{35}$$
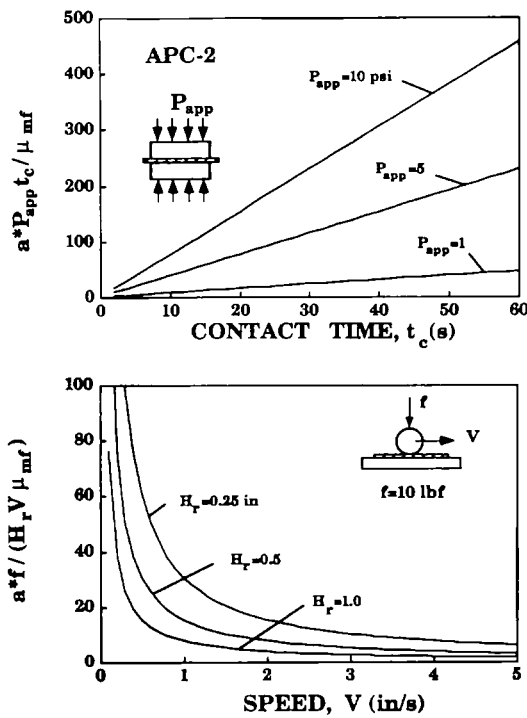

Figure 11. *Values of the dimensionless parameters in the intimate contact models for the press [Equation (36)] and for the tape layer [Equation (41)].*

The degree of intimate contact can be calculated by either Equation (33) or Equation (34). In the special case when the temperature and pressure are constant during time t_c, the expression for the degree of intimate contact becomes

$$D_{ic} = \frac{1}{w^*}\left[1 + a^*\frac{P_{app}}{\mu_{mf}}t_c\right]^{1/5}$$

(36)

For the tape laying process, P_{app} is the pressure applied by the roller to the composite (Figure 12). Under an applied force f the roller is in contact with the composite through an arc length $g - h$ (Figure 12). The linear distance between points g and h is denoted by l_c. While the roller travels this small l_c distance, the temperature can be assumed to be nearly constant from g to h. When this assumption is valid, the viscosity μ_{mf} is constant. Then the integral in Equations (33) and (34) can be written as

$$\int_0^{t_c} \frac{P_{app}}{\mu_{mf}}dt = \frac{1}{\mu_{mf}}\int_0^{t_c} P_{app}dt$$

(37)

where t_c is the contact time, which is the time it takes for the roller to travel the distance l_c

$$t_c = \frac{l_c}{V}$$

(38)

where V is the roller speed. By assuming that the arc between g and h is shallow, the force balance in the vertical direction is

$$f \approx \int_0^{H_r} \int_0^{l_c} P_{app}dxdy$$

(39)

where H_r is the width of the roller. Since $x = Vt$, Equation (37) can be integrated to yield

$$\frac{1}{\mu_{mf}}\int_0^{t_c} P_{app}dt = \frac{f}{\mu_{mf}VH_r}$$

(40)

The degree of intimate contact Equation (33) now becomes

$$D_{ic} = \frac{1}{w^*}\left[1 + a^*\frac{f}{\mu_{mf}VH_r}\right]^{1/5} \quad \text{tape laying}$$

(41)

For the filament winding process, P_{app} is the pressure applied by the roller to
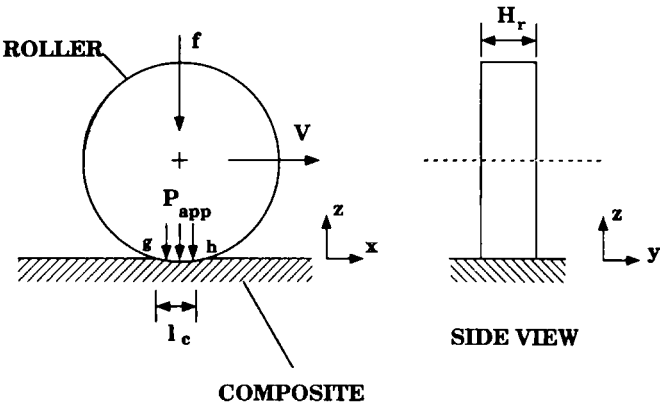
Figure 12. *Interaction of the roller and the composite in tape laying.*

the composite (see Figure 13). Following the same assumptions as in the tape laying process, the degree of intimate contact for filament winding may be calculated by the expression

$$D_{ic} = \frac{1}{w^*}\left[1 + a^*\frac{f}{\mu_{mf}\omega r_c H_r}\right]^{1/5} \qquad \text{filament winding} \qquad (42)$$

where ω is the speed at which the mandrel rotates, H_r is the width of the roller, and r_c is the radius of the cylinder at the interface at which the degree of intimate contact is being evaluated. Interestingly, Equations (41) and (42) do not require

Figure 13. *Interaction of the roller and the composite in filament winding.*

a knowledge of either the contact length l_c or the contact time t_c. These equations only contain the geometry of the ply a_o, b_o, w_o, the roller width H_r, the speed V or ω, the applied force f, and the viscosity μ_{mf} directly under the roller at the interface at which the degree of intimate contact is being evaluated.
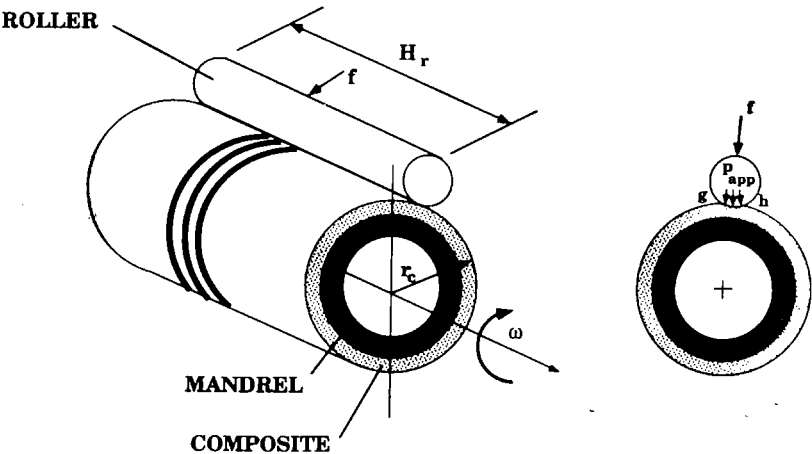
Bonding

After intimate contact has been established at any point on the interface, the bonding process starts. It has been suggested (e.g., References [2, 6, and 22–24]) that bonding is caused mostly by autohesion. The degree of autohesion can be approximated by the expression

$$D_{au} = kt_a^{n_a} \tag{43}$$

where t_a is the time elapsed from the start of the autohesion process, and $\varkappa$ is a constant which depends on temperature. The exponent n_a is a constant. The degree of bonding can now be expressed as

$$D_b = (D_{ic})(D_{au}) \tag{44}$$

At a given location, the degree of bonding at time t can then be calculated by [2]

$$
\begin{aligned}
(D_b)_{at\,t} &= [(D_{ic})_{at\,\Delta t} - (D_{ic})_{at\,0}][D_{au}|_{\Delta t}^t] \\
&+ [(D_{ic})_{at\,2\Delta t} - (D_{ic})_{at\,\Delta t}][D_{au}|_{2\Delta t}^t] + \ldots
\end{aligned}
\tag{45}
$$

where Δt is an arbitrary time step. $D_{au}|_{i\Delta t}^t$ is the change in the degree of autohesion from the ith time step to time t

$$D_{au}|_{i\Delta t}^t = D_{au}^t - D_{au}^{i\Delta t} \tag{46}$$

At time t_a the degree of autohesion $D_{au}^{t_a}$ is defined as [6]

$$D_{au}^{t_a} = \sum_{j=1}^{t_a/\Delta t} (\bar{\varkappa} t_{j+1}^{n_a} - \bar{\varkappa} t_j^{n_a}) \tag{47}$$

where $t_j^{n_a}$ and $t_{j+1}^{n_a}$ are the time at the j and $j + 1$ time steps, respectively. $\bar{\varkappa}$ is evaluated at the mean temperature of the j and $j + 1$ time steps. In some processes autohesion proceeds much faster than intimate contact. In this case Equation (44) reduces to

$$D_b \approx D_{ic} \tag{48}$$

and Equation (45) becomes

$$
\begin{aligned}
(D_b)_{at\,t} &\approx [(D_{ic})_{at\,\Delta t} - (D_{ic})_{at\,0}] \\
&+ [(D_{ic})_{at\,2\Delta t} - (D_{ic})_{at\,\Delta t}] + \ldots
\end{aligned}
\tag{49}
$$

Multiple Passes

During tape laying and filament winding, the roller generally makes more than one pass over a given area. From one pass to the next, the thickness of the composite at the same location may change. Thus, at each pass, an interface may experience different pressures and temperatures even though the applied heat and pressure remain the same. When calculating consolidation and bonding, the effects of these sequential passes must be taken into account by sequentially applying the above consolidation and bonding models. At each pass of the roller, consolidation and bonding must be calculated taking into account the previous consolidation and bonding history and the temperature which currently exists at the relevant interface. This implies that in the case of multiple passes, integration [in Equation (33)] is performed over the elapsed total time. Since pressure is only applied over discrete time intervals (t_{c1}, t_{c2}, etc.), the integral in Equation (33) is replaced by

$$\int_0^{t_c} \frac{P_{app}}{\mu_{mf}} dt = \int_0^{t_{c1}} \frac{P_{app}}{\mu_{mf}} dt + \int_0^{t_{c2}} \frac{P_{app}}{\mu_{mf}} dt + \ldots \tag{50}$$

where μ_{mf} is the viscosity corresponding to the temperature which exists at the interface during the time of contact.

5. STRESS-STRAIN SUBMODEL

The stress-strain submodel provides the stresses and strains introduced in the composite during processing. For a flat plate the straightforward results of laminate plate theory can be used [25–27]. For a cylinder, the analysis of Lee and Springer [19], developed for thermosetting matrix composites, can be used with one modification. The degree of cure α in the Lee and Springer analysis must be replaced by the crystallinity c. For details of the analysis the reader is referred to Reference [19]. It is only noted here that this analysis applies to cylinders in which the stresses and strains vary only in the radial direction.

6. METHOD OF SOLUTION

Solutions to the thermochemical, consolidation and bonding, and stress and strain sub-models must be obtained by numerical methods. The solution procedures are summarized below. As was noted before, the different submodels are interrelated and must be solved simultaneously.

Solutions to the thermochemical submodel were obtained by finite element methods [29,30]. The following elements were used (Chapters 2 and 3 in Reference [29], and Chapters 3 and 4 in Reference [30]): a two node linear element, a four node bilinear quadrilateral element, a two node linear axisymmetric element in polar coordinates, and a four node bilinear quadrilateral element in polar

coordinates. The solution algorithm for the energy equation was implicit back-ward Euler (Chapters 7 and 8 in Reference [29]). The crystallinity was calculated at each time step using an implicit finite difference solution of Equa-tion (6) [31].

The consolidation and bonding submodels were evaluated by direct solution of Equations (33) and (45), respectively.

In the stress and strain submodel, the boundary conditions were written so that the matrix of coefficients formed a doubly bordered band diagonal matrix. This system of equations was solved by the algorithm developed by Lee [32].

Computer Codes

Four computer codes were written which implement the aforementioned solu-tion procedures. All these codes are "user friendly" and can readily be used to generate numerical results of different problems of practical interest. The types of problems which can be solved with each code are as follows.

The PLASTIC2 code describes processing in an autoclave or in a press in which the applied pressures and temperatures are uniform (Figure 1). This code is an extension of Lee and Springer's PLASTIC code [2]. The original PLASTIC code was extended to allow for heating as well as cooling of the plate and to include the calculation of thermal stresses and strains. The new bonding model proposed in this investigation is also included in the code.

The PL-TAPE code simulates the tape laying process.

The PL-WIND1 code describes the filament winding process in the case when temperature and crystallinity vary only in the radial direction. The PL-WIND2 code simulates the filament winding of cylinders in which the temperature, crystallinity, and bonding may vary in the radial and circumferential directions. Note, even in this case, the stress and strains are taken to vary only radially.

The input required by each code and the output provided by each code are sum-marized in Tables 1, 2, 3, and 4.

7. CONCLUDING REMARKS

The models and the computer codes developed in this investigation can be used to calculate the thermal and mechanical behavior of thermoplastic composites during processing in an autoclave or press, by tape laying, and by filament wind-ing. Specifically, the computer codes provide the interply temperature, the crystallinity, the viscosity, the degree of intimate contact, the degree of bonding, and the residual stresses and strains in the composite. With this information the codes can be used to assess the usefulness of each manufacturing process for a given application and to establish the appropriate processing conditions in the manner discussed in Reference [33].

The computer codes PLASTIC2, PL-TAPE, PL-WIND1, and PL-WIND2 de-veloped in this study have user friendly interfaces. The emphasis in writing these codes was on generating results. No special effort was made to optimize the code, to minimize storage requirements, or to increase the computing speed. Presently, for a 16 ply thick, 12 in long laminate the calculation requires about 30 minutes

Table 1. Input parameters required for the PLASTIC2 code.

A. Thermochemical Submodel

- thickness of the platens H_{pb} and H_{pt}
- thickness of each composite layer Δz
- fiber volume fraction of the layer ν_f
- fiber, matrix, and platen density ϱ_f, ϱ_m, ϱ_p
- fiber, matrix, and platen specific heat C_f, C_m, C_p
- fiber, matrix, and platen thermal conductivity k_f, k_m, k_p
- theoretical ultimate heat of crystallinity H_u
- a relationship between the change in matrix crystallinity dc/dt and the heating or cooling rate dT/dt, and the temperature T
- a relationship between the matrix viscosity μ_m and the temperature T
- initial crystallinity in the composite c_{in}
- applied temperature T_t or heat flux q_t at the top platen surface; or applied temperature at the top composite surface T_{st}
- applied temperature T_b or heat flux q_b at the bottom platen surface; or applied temperature at the bottom composite surface T_{sb}

B. Consolidation and Bonding Submodels

- geometric ratios a_o/b_o and w_o/b_o
- a relationship between the matrix fiber viscosity μ_{mf} and the temperature T
- the gauge pressure applied to the plate P_{app}
- the composite temperature history (from the thermochemical submodel)
- autohesion constants κ and n_a

C. Stress and Strain Submodel

- composite on axis engineering constants E_{xx}, E_{yy}, G_{xy}, ν_{xy}
- composite on axis thermal expansion coefficients β_{xx} and β_{yy}
- composite on axis chemical shrinkage coefficients η_{xx} and η_{yy}
- composite temperature history (from the thermochemical submodel)
- lowest temperature at which the laminate is in a stress free state T_l

---

Table 2. Input parameters required for the PL-TAPE code.

A. Thermochemical Submodel

- thickness of the tool plate H_{pb}
- length of the tool plate L
- thickness of each composite layer Δz
- matrix mass fraction of the layer m_m
- fiber, matrix, and tool plate density $\varrho_f,\ \varrho_m,\ \varrho_p$
- fiber, matrix, and tool plate specific heat $C_f,\ C_m,\ C_p$
- fiber, matrix, and tool plate thermal conductivity $k_f,\ k_m,\ k_p$
- theoretical ultimate heat of crystallinity H_u
- a relationship between the change in matrix crystallinity *dc/dt* and the heating or cooling rate *dT/dt*, and the temperature T
- a relationship between the matrix viscosity μ_m and the temperature T
- initial crystallinity in the composite c_{in}
- applied temperature or heat flux at the top composite surface (T_{st} or q_{st})
- applied temperature or heat flux along the two composite edges (T_{se} or q_{se})
- applied temperature or heat flux at the bottom tool plate surface (T_b or q_b); or applied temperature at the bottom composite surface T_{sb}
- speed of the head V

B. Consolidation and Bonding Submodels

- geometric ratios a_o/b_o and w_o/b_o
- a relationship between the matrix fiber viscosity μ_{mf} and the temperature T
- either the head speed V, roller force f, and width of the roller H_r or the applied roller pressure P_{app}
- a relationship between the prescribed composite surface temperature T_{st} (or heat flux q_{st}) and the roller force f or the pressure P_{app}
- the composite temperature history (from the thermochemical submodel)
- autohesion constants x and n_a

C. Stress and Strain Submodel

- composite on axis engineering constants $E_{xx},\ E_{yy},\ G_{xy},\ \nu_{xy}$
- composite on axis thermal expansion coefficients β_{xx} and β_{yy}
- composite on axis chemical shrinkage coefficients η_{xx} and η_{yy}
- composite temperature history (from the thermochemical submodel)
- lowest temperature at which the laminate is in a stress free state T_f

Table 3. Input parameters required for the PL-WIND1 and PL-WIND2 codes.

A. Overall Geometry
- cylinder length L
- radius of mandrel inner surface r_i
- radius of mandrel outer surface r_m
- total number of composite layers wound n_c^l

B. Winding Parameters
- bandwidth of the tow W_t
- mandrel angular velocity ω
- winding angle ϕ_0
- initial fiber tension F_0

C. Thermochemical Submodel
- thickness of each layer in the composite cylinder Δr
- matrix mass fraction m_m
- fiber, matrix, and mandrel density ϱ_f, ϱ_m, ϱ_{man}
- fiber, matrix, and mandrel specific heat C_f, C_m, C_{man}
- fiber, matrix, and mandrel thermal conductivity k_f, k_m, k_{man}
- theoretical ultimate heat of crystallinity H_u
- a relationship between the change in matrix crystallinity dc/dt and the heating or cooling rate dT/dt, and the temperature T
- a relationship between the matrix viscosity μ_m and the temperature T
- initial crystallinity in the composite c_{in}
- applied temperature or heat flux at the outer composite surface (T_{so} or q_{so})
- applied temperature or heat flux at the inner mandrel surface (T_{si} or q_{si})

D. Consolidation and Bonding Submodels
- geometric ratios a_o/b_o and w_o/b_o
- a relationship between matrix fiber viscosity μ_{mf} and the temperature T
- the composite temperature history (from the thermochemical submodel)
- the applied pressure at the composite outer surface P_{app} (PL-WIND1 only)
- either the roller force f or the applied roller pressure P_{app} (PL-WIND2 only)
- a relationship between the prescribed composite outer surface temperature T_{so} (or heat flux q_{so}) and the roller force f or the pressure P_{app} (PL-WIND2 only)
- autohesion constants x and n_a

E. Stress and Strain Submodel
- composite longitudinal and transverse moduli E_{xx}, E_{yy}, E_{zz}
- composite longitudinal and transverse Poisson's ratios ν_{xy}, ν_{yz}, ν_{xz}
- composite shear moduli G_{xy}, G_{yz}, G_{xz}
- composite longitudinal and transverse thermal expansion coefficients β_{xx}, β_{yy}, β_{zz}
- composite longitudinal and transverse chemical shrinkage coefficients η_{xx}, η_{yy}, η_{zz}
- mandrel Young's modulus E_{man}
- mandrel Poisson's ratio ν_{man}
- mandrel thermal expansion coefficient β_{man}
- composite temperature history (from the thermochemical submodel)

Table 4. Output from PLASTIC2, PL-TAPE, PL-WIND1, and PL-WIND2 codes.

- the temperature inside the composite T
- the matrix viscosity μ_m or fiber matrix viscosity μ_{mf} inside the composite during processing
- the crystallinity c of the composite
- the degree of intimate contact D_{ic} between composite layers
- the degree of bonding D_b of composite layers
- the residual stresses σ and strains ϵ in the composite

cpu time on a Sun 4 SPARC work station for PL-TAPE. This time could possibly be reduced by streamlining the code and by using computers with higher processing speeds.

Data pertaining to processing of thermoplastic composites in a press or in a tape laying apparatus are given in a companion paper [34].

8. ACKNOWLEDGEMENTS

9. APPENDIX A

Crystallinity and Viscosity of PEEK 150P Polymer and APC-2/AS4

For PEEK empirical expressions relating the measured rate of crystallization to the temperature have been proposed by several researchers [1–3,28,35–39]. The expressions proposed by Lee and Springer [2], Velisaris and Seferis [1,3] and Maffezzoli and his coworkers [21] have been incorporated into the thermochemical submodel.

The rate of change in crystallinity is related to the crystallinity, the temperature, and the change in temperature by an expression of the form [Equation (6)]

$$\frac{dc}{dt} = f_1\left(c, T, \frac{dT}{dt}\right) \tag{A1}$$

During heating $(dT/dt \geq 0)$, we adopt the expression for f_1 proposed by Maffezzoli et al. [21] shown in Table A-1. During cooling $(dT/dt < 0)$, the expression for f_1 proposed by Lee and Springer [2] or Velisaris and Seferis [1,3] may be applied. These expressions are given in Tables A-2 and A-3, respectively.

The matrix viscosity of PEEK μ_m [2] and matrix fiber viscosity of APC-2/AS4 μ_{mf} are given in Table A-4.

10. APPENDIX B

Variation of Material Properties with Crystallinity and Temperature

During manufacturing the mechanical and thermal properties of the composite

Table A-1. Crystallinity function f_t for APC-2/AS4 during heating [21].

n	**0.5**
E_a (KJ/mol)	**397**
K_0 (s^{-1})	5.05 E31

$$\frac{dc}{dt} = -c_{in}\frac{dX_t}{dt}$$

$$\frac{dX_t}{dt} = K(1 - X_t)^n$$

$$X_t = (c_{in} - c)/c_{in}$$

$$K = K_0 \exp(E_a/RT)$$

where c_{in} is the initial crystallinity.

Table A-2. Crystallinity function f_t for APC-2/AS4 during cooling [2].

A_1	-0.03
A_2	0.42
A_3 (1/K)	-0.037
A_4	11.3
n	0.8
H_u (J/g)	130.0

$$\frac{dc}{dt} = \frac{H_t}{H_u}\frac{dc_r}{dt}$$

$$\frac{H_t}{H_u} = A_1 \ln\left(\frac{dT}{dt}\right) + A_2$$

$$\frac{dc_r}{dt} = -(1 - c_r)\frac{(d\phi/dT)}{(dT/dt)^{n-1}}$$

$$\phi = \exp(A_3 T + A_4)$$

where dT/dt is the cooling rate in K/min.

Table A-3. Crystallinity function f, for APC-2/AS4 during cooling [1,3].

T_g (K)	367
n_1	2.5
T_{m1} (K)	593
C_{11} (s^{-n}K^{-1})	2.08 × 10^{10}
C_{21} (K)	4050
C_{31} (K^3)	1.8 × 10^7
W_1	0.61
n_2	1.5
T_{m2} (K)	615
C_{12} (s^{-n}K^{-1})	2.08 × 10^{10}
C_{22} (K)	7600
C_{32} (K^3)	3.2 × 10^6

$$\frac{dc}{dt} = c_\infty \frac{d}{dt}(W_1 F_{vc1} + W_2 F_{vc2})$$

$$W_1 + W_2 = 1$$

$$F_{vci} = 1 - \exp\left[-C_{1i} \int_0^{t_i} T \exp\{ -[C_{2i}/(T - T_g + 51.6) \right.$$

$$\left. + C_{3i}/(T(T_{mi} - T)^2)]\} n_i t_i^{(n_i - 1)} dt_i \right] \qquad \text{where } i = 1,2$$

where c_∞ is the equilibrium volume fraction crystallinity and T is the temperature in K.

Table A-4. Viscosity of PEEK 150P polymer and APC-2/AS4.

$$\mu_m = 1.13\text{E} - 10\left(\exp\frac{19,100}{T \text{ (K)}}\right) \quad \text{Pa·s}$$

$$\mu_{mf} = 132.95\left(\exp\frac{2969}{T \text{ (K)}}\right) \quad \text{Pa·s}$$

The value of μ_{mf} was provided by the manufacturer.

vary. When changes in the composite's properties during melting and crystallinity are not known accurately, the composite properties may be expressed either as a function of crystallinity or as a function of temperature.

The variation of a material property Y which varies with crystallinity may be approximated by [39]

$$Y = Y_1 + Y_2 c + Y_3 c^2 \tag{B1}$$

where Y is the composite property, Y_i $(i = 1,2,3)$ is a constant for the given property and c is the crystallinity.

The variation of a material property with temperature may be described by the following piecewise approximation [40]

$$
\begin{aligned}
Y &= Y^g & T &< T_g \\
Y &= \bar{y} Y^m + (1 - \bar{y}) Y^g & T_g &\leq T \leq T_m \\
Y &= Y^m & T_m &< T
\end{aligned}
\tag{B2}
$$

where T is the composite temperature, the subscripts g and m refer to the property values below the matrix glass transition temperature and above the matrix melt temperature, respectively. The ratio $\bar{y}$ is defined as

$$\bar{y} = \frac{T - T_g}{T_m - T_g} \tag{B3}$$

The above properties vary with time since the crystallinity and temperature vary with time.

REFERENCES

1. Seferis, J. C. and C. N. Velisaris. 1986. "Modeling-Processing-Structure Relationships of Polyetheretherketone (PEEK) Based Composites," *Materials Sciences for the Future*. Society for the Advancement of Material and Process Engineering. pp. 1236–1252.

2. Lee, W. I. and G. S. Springer. 1987. "A Model of the Manufacturing Process of Thermoplastic Matrix Composites," *Journal of Composite Materials*, 21:1017–1055.

3. Velisaris, C. N. and J. C. Seferis. 1988. "Heat Transfer Effects on the Processing-Structure Relationships of Polyetheretherketone (PEEK) Based Composites," *Polymer Engineering and Science*, 28:583–591.

4. Muzzy, J., L. Norpoth and B. Varughese. 1989. "Characterization of Thermoplastic Composites for Processing," *SAMPE Journal*, 25(1):23–29.

5. Hwang, S. J. and C. L. Tucker, III. 1990. "Heat Transfer Analysis of Continuous Fiber/Thermoplastic Matrix Composites during Manufacture," *Journal of Thermoplastic Composite Materials*, 3:41–51.

6. Loos, A. C. and M.-C. Li. 1990. "Heat Transfer Analysis of Compression Molded Thermoplastic Composites," *Advanced Materials: The Challenge for the Next Decade*. Society for the Advancement of Material and Process Engineering, pp. 557–570.

7. Gruber, M. B. 1986. "Thermoplastic Tape Laydown and Consolidation," Society of Manufacturing Engineers, Paper No. EM86-905.

8. Beyeler, E. P. and S. I. Guceri. 1988. "Thermal Analysis of Laser Assisted Thermoplastic Matrix Composite Tape Consolidation," *Journal of Heat Transfer*, 110:424–430.

9. Grove, S. M. 1988. "Thermal Modelling of Tape Laying with Continuous Carbon-Fibre-Reinforced Thermoplastic," *Composites*, 19:367–375.

10. Andersen, B. J. and J. S. Colton. 1989. "A Study in the Lay-up and Consolidation of High Performance Thermoplastic Composites," *Tomorrow's Materials: Today*. Society for the Advancement of Material and Process Engineering, 34:1952–1963.

11. Andersen, B. J. and J. S. Colton. 1990. "Automation of Thermoplastic Composite Processing," *Journal of Composite Materials*, 24:150–174.

12. Nejhad, M. N., R. D. Cope and S. I. Guceri. 1991. "Thermal Analysis of In-situ Thermoplastic Composite Tape Laying," *Journal of Thermoplastic Composite Materials*, 4:20–45.

13. Cirino, M. 1989. "Axisymmetric and Cylindrically Orthotropic Analysis of Filament Winding," Ph.D. Thesis, University of Delaware, Newark, DE.

14. Brage, A. and C. Lamrell. 1988. "Heat Flow Analysis in Connection with Thermoplastic Filament Winding," *SAMPE Quarterly*, 19(3):31–35.

15. Beyeler, E. P. 1987. "Melting and Solidification in Processing and Applications to Thermoplastic Matrix Composites Manufacturing," Ph.D. Thesis, University of Delaware, Newark, DE.

16. Beyeler, E. P. and S. I. Guceri. 1988. "Experimental Investigation of Laser Assisted Thermoplastic Tape Consolidation," *Journal of Composite Materials*, 1:107–121.

17. Nejhad, M. N., R. D. Cope and S. I. Guceri. In press. "Thermal Analysis of In-Situ Thermoplastic-Matrix Composite Filament Winding," *Journal of Heat Transfer*.

18. Loos, A. C. and G. S. Springer. 1983. "Curing of Epoxy Matrix Composites," *Journal of Composite Materials*, 17:135–169.

19. Lee, S. Y. and G. S. Springer. 1990. "Filament Winding Cylinders: I. Process Model," *Journal of Composite Materials*, 24:1270–1298.

20. Calius, E. P. and G. S. Springer. 1990. "A Model of Filament-Wound Thin Cylinders," *International Journal of Solids and Structures*, 26:271–297.

21. Maffezzoli, A. M., J. M. Kenny and L. Nicolais. 1989. "Welding of Peek/Carbon Fiber Composite Laminates," *SAMPE Journal*, 25(1):35–39.

22. Dara, P. H. and A. C. Loos. 1985. "Thermoplastic Matrix Composite Processing Model," Center for Composite Materials and Structures, Report No. CCMS-85-10, Virginia Polytechnic Institute and State University, Blacksburg, VA.

23. Li, M. C. and A. C. Loos. 1990. "Autohesion Model for Thermoplastic Composites," Center for Composite Materials and Structures, Report No. CCMS-90-03, Virginia Polytechnic Institute and State University, Blacksburg, VA.

24. Howes, J. C. and A. C. Loos. 1987. "Interfacial Strength Development in Thermoplastic Resins and Fiber Reinforced Thermoplastic Composites," Center for Composite Materials and Structures, Report No. CCMS-87-15, Virginia Polytechnic Institute and State University, Blacksburg, VA.

25. Jones, R. M. 1975. *Mechanics of Composite Materials*, Scripta Book Company, pp. 193–198.

26. Lee, W. I., P. R. Ciriscioli and G. S. Springer. 1986. "Dimensional Stability of Unsymmetric Laminates," *Materials Sciences for the Future*, Society for the Advancement of Material and Process Engineering, pp. 750–763.

27. Tsai, S. W. 1987. Chapter 15 in *Composites Design*, Think Composites.

28. Ozawa, T. 1971. "Kinetics of Non-Isothermal Crystallization," *Polymer*, 12:150–158.

29. Hughes, T. J. R. 1987. *The Finite Element Method*. Prentice-Hall, Inc.

30. Reddy, J. N. 1984. *An Introduction to the Finite Element Method*. McGraw-Hill, Inc.

31. Ferziger, J. H. 1981. Chapter 3 in *Numerical Methods for Engineering Application*. John Wiley & Sons.

32. Lee, S.-Y. 1989. "Filament Winding Process Model," Ph.D. Thesis, Department of Civil Engineering, Stanford University, Stanford, CA.

33. Ciriscioli, P. R. and G. S. Springer. 1990. *Smart Autoclave Cure of Composites*. Lancaster, PA: Technomic Publishing Co., Inc.

34. Mantell, S. C., Q. Wang and G. S. Springer. Submitted. "Processing Thermoplastic Composites in a Press and by Tape Laying—Experimental Results," *Journal of Composite Materials*.

35. Blundell, D. J. and B. N. Osborn. 1983. "The Morphology of Poly(aryl-ether-ether-ketone)," *Polymer*, 24:953–958.

36. Blundell, D. J., J. M. Chalmers, M. W. MacKenzie and W. F. Gaskin. 1985. "Crystalline Morphology of the Matrix of PEEK-Carbon Fiber Aromatic Polymer Composites. I. Assessment of Crystallinity," *SAMPE Quarterly*, 16(4):22–30.

37. Blundell, D. J. and B. N. Osborn. 1985. "Crystalline Morphology of the Matrix of PEEK-Carbon Fiber Aromatic Polymer Composites. II. Crystalline Behavior," *SAMPE Quarterly*, 17(1):1–6.

38. Cebe, P. and S. D. Hong. 1986. "Crystallization Behaviour of Poly(ether-ether-ketone)," *Polymer*, 27:1183–1192.

39. Talbott, M. F., G. S. Springer and L. A. Berglund. 1987. "The Effects of Crystallinity on the Mechanical Properties of PEEK Polymer and Graphite Fiber Reinforced PEEK," *Journal of Composite Materials*, 21:1056–1081.

40. Cogswell, F. N. 1987. "The Processing Science of Thermoplastic Structural Composites," *International Polymer Processing*, pp. 157–165.